

Neutron stars as photon double-lenses: constraining resonant conversion into ALPs

Kyrylo Bondarenko,^{1,2,3,*} Alexey Boyarsky,^{4,†} Josef Pradler,^{5,‡} and Anastasia Sokolenko^{6,7,§}

¹*IFPU, Institute for Fundamental Physics of the Universe, via Beirut 2, I-34014 Trieste, Italy*

²*SISSA, via Bonomea 265, I-34132 Trieste, Italy*

³*INFN, Sezione di Trieste, SISSA, Via Bonomea 265, 34136, Trieste, Italy*

⁴*Institute Lorentz, Leiden University, Niels Bohrweg 2, Leiden, NL-2333 CA, the Netherlands*

⁵*Institute of High Energy Physics, Austrian Academy of Sciences, Georg-Coch-Platz 2, 1010 Vienna, Austria*

⁶*Theoretical Astrophysics Department, Fermi National Accelerator Laboratory, Batavia, Illinois, 60510, USA*

⁷*Kavli Institute for Cosmological Physics, The University of Chicago, Chicago, IL 60637, USA*

(Dated: March 17, 2022)

Axion-photon conversion is a prime mechanism to detect axion-like particles that share a coupling to the photon. We point out that in the vicinity of neutron stars with strong magnetic fields, magnetars, the effective photon mass receives comparable but opposite contributions from free electrons and the radiation field. This leads to an energy-dependent resonance condition for conversion that can be met for arbitrary light axions and leveraged when using systems with detected radio component. Using the magnetar SGR J1745-2900 as an exemplary source, we demonstrate that sensitivity to $|g_{a\gamma}| \sim 10^{-12} \text{ GeV}^{-1}$ or better can be gained for $m_a \lesssim 10^{-6} \text{ eV}$, with the potential to improve current constraints on the axion-photon coupling by more than one order of magnitude over a broad mass range. With growing insights into the physical conditions of magnetospheres of magnetars, the method hosts the potential to become a serious competitor to future experiments such as ALPS-II and IAXO in the search for axion-like particles.

Introduction. Axions, originally introduced as a solution to the strong CP-problem of QCD [1–8], with the additional benefit of serving as dark matter (DM) candidates [9–11] are now broader appreciated as low-energy messengers of high-scale new physics. For example, in string constructions, axion-like particles (ALPs) appear in multitude [12–18], populating a great range of masses m_a and couplings, representing viable targets for astronomical and laboratory-based searches [19–23]. Cumulatively, the largest efforts have gone into probing the axion-photon coupling. Here, once the axion mass is below the μeV scale, the leading probes are from high energy astrophysics: axions can be produced in stars or supernovae [24, 25] and subsequently convert into X- and γ -rays in galactic magnetic fields [26–28]. Alternatively, photon-ALP oscillations can leave their imprint on high energy photon spectra, e.g. leading to the dimming of sources [29–32], or, sometimes, even explain their brightness [33, 34].

Some of the strongest constraints limiting the axion-photon coupling to $|g_{a\gamma}| \lesssim 10^{-12} \text{ GeV}^{-1}$ have been placed from *non-resonant* conversion using well-measured spectra of radio galaxies, such as from NGC 1275 in the Perseus cluster [35, 36] and M87 [37] in the Virgo cluster. In turn, *resonant* conversion has been used to search for axion DM through radio lines produced in the conversion to photons using the strong magnetic fields of neutron stars (NS) [38–44], and significant recent effort is being invested in pinning down the physical circumstances of signal formation [45–47]. Of central importance to these studies is the account of the medium-dependent mixing between photons and ax-

ions [48]. Photons experience a modification of their dispersion relation in media that may be cast in terms of an effective mass m_{eff} . As is well known, the forward scattering on free, non-relativistic charges leads to a positive, energy-independent contribution $m_{\text{eff}}^2|_{\text{charge}} \simeq \omega_p^2$, where ω_p is the plasma frequency [49]. Resonant conversion becomes possible when $m_a^2 = m_{\text{eff}}^2$, and is hence believed to be relevant only in a narrow range of ALP mass where $m_a^2 = \omega_p^2$ is met along the propagation path associated with significant conversion probability.

The purpose of this paper to point out that *resonant* conversion is possible over a large range in m_a , considerably improving the sensitivity to $g_{a\gamma}$ and independent of the condition that ALPs constitute DM. The central observation is that photons also receive an energy-dependent, negative contribution to their dispersion relation from the background radiation field [50], $m_{\text{eff}}^2|_{\text{EM}}(\omega) < 0$, where ω is a photon energy. This has important ramifications for photon-ALP conversion: because the contribution grows in magnitude with photon energy as ω^2 , the resonance condition $m_a^2 = m_{\text{eff}}^2(\omega)$ that can eventually be met for *any* axion mass $m_a \leq \omega_p$. In the magnetospheres of NS with the strongest magnetic fields, magnetars, this condition is met for radio frequencies (GHz-THz) close to the surface. As the strength of resonances increases with energy, the flux of photons can reduce significantly. Together with the presence of a geometric boundary given by the NS surface, this imprints a sharp spectral feature that can be searched for in radio data. Our objective here is to point out the main ideas and study the principal sensitivity to $g_{a\gamma}$. It is to be followed up by more detailed analyses of the involved

arXiv:2203.08663v1 [hep-ph] 16 Mar 2022

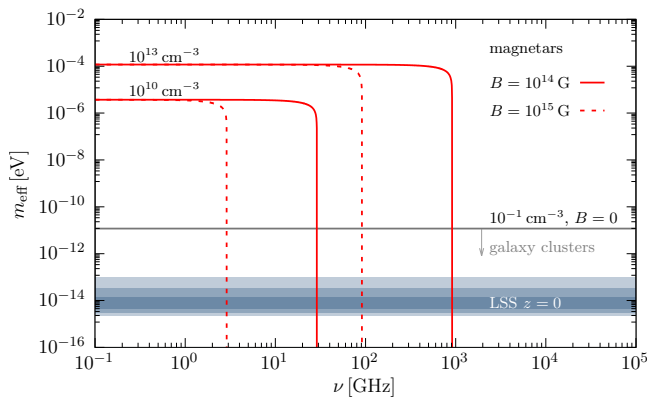


FIG. 1. Real branch of the effective photon mass as a function of photon frequency ν and electron densities as labeled. The solid (dashed) red lines represent a neutron star environment with $B = 10^{14}$ G (10^{15} G). For comparison, the gray horizontal line shows a typical galaxy cluster central density [52]. The 1σ - 3σ shaded bands are inferred from the free electron distribution of the large scale structure at $z = 0$ [53].

stellar systems [51].

The paper is organized as follows. First, we establish the resonance conditions and the expected photon flux. We then demonstrate our ideas using the radio measurements of the magnetar SGR J1745-2900 close to the Galactic center before concluding.

Resonant axion conversion. Axion-like particles a interact with photons through the effective Lagrangian,

$$\mathcal{L}_{\text{int}} = -\frac{g_{a\gamma}}{4} a F_{\mu\nu} \tilde{F}^{\mu\nu} = g_{a\gamma} \vec{E} \cdot \vec{B}, \quad (1)$$

where $F_{\mu\nu}$ ($\tilde{F}^{\mu\nu}$) is the (dual) photon field strength; $g_{a\gamma}$ and m_a are the only other relevant model parameters. For the QCD axion $g_{a\gamma} \sim \alpha/(\pi f_a)$ and $m_a \approx m_\pi f_\pi/f_a$ holds, whereas for ALPs one keeps m_a as a free parameter while $g_{a\gamma}^{-1}$ is still expected to be informative on the UV scale f_a of symmetry breaking; we use the term axion and ALP interchangeably. In a magnetic field \vec{B} the interaction (1) enables the conversion of photons (with electric field \vec{E}) into axions and vice versa [48, 54, 55]. If the condition $m_a^2 = m_{\text{eff}}^2$ is satisfied along the photon's path, such conversion becomes resonant.

The resonance condition is naturally met several times, as the background medium typically undergoes spatial variations on small scales on top of an overall varying trend; see e.g. [53, 56, 57]. The net result is that the photon and axion populations are driven towards equipartition. When both photon polarization degrees of freedom participate in the mixing, it yields the smallest and hence most conservative overall photon-to-axion conversion probability [58],

$$P_{\text{tot}} \approx \frac{1}{3} (1 - e^{-3P_{\text{lin}}}), \quad P_{\text{lin}} = \frac{\pi g_{a\gamma}^2 \omega}{m_a^2} \sum_i B_{T,i}^2 R_i. \quad (2)$$

Here, P_{lin} is found from the Landau-Zener transition probability, $B_{T,i} = B_T(\ell_i)$ is the component of the magnetic field orthogonal to the direction of photon/axion propagation and $R_i = |d \ln m_{\text{eff}}^2 / d\ell|_{\ell=\ell_i}^{-1}$ is the scale parameter with ℓ being the distance along the line-of-sight; negligible redshift has been assumed. The derivative of R is calculated at each point of resonance $m_a^2 = m_{\text{eff}}^2(\ell_i)$. The loss of photons into axions is imprinted onto an initial photon flux $F_{\text{in}}(\omega)$ as,

$$F_{\text{obs}}(\omega) = F_{\text{in}}(\omega)[1 - P_{\text{tot}}(\omega)]. \quad (3)$$

For unpolarized sources, the effective photon mass receives two important contributions (“double lens”),

$$m_{\text{eff}}^2 = \omega_p^2 - m_{\text{eff}}^2|_{\text{EM}}, \quad m_{\text{eff}}^2|_{\text{EM}} = \frac{88\alpha^2\omega^2}{135m_e^4} \rho_{\text{EM}}, \quad (4)$$

where $\omega_p^2 = 4\pi\alpha n_e/m_e$. The second, negative term is the photon-photon scattering contribution $m_{\text{eff}}^2|_{\text{EM}}$ of the radiation field [50]. It implies that the resonance condition $m_a^2 = m_{\text{eff}}^2$ can eventually be met for *any* axion mass satisfying $m_a \leq \omega_p$. This observation is instrumental to our proposal.

Before proceeding, we emphasize that the applicability of (2) and hence the formulation of resonant conversion requires a well-separated two-level system away from the resonance point, i.e., an off-diagonal mixing that is much smaller than its diagonals in the Hamiltonian. This translates into the condition $\epsilon \equiv 2|g_{a\gamma} B_{T,i} \omega / |m_{\text{eff}}^2(\ell) - m_a^2| \ll 1$ for $|\ell - \ell_i| \gg 0$ and it guides the selection of potential sources and frequency bands for observing axion-photon conversion. If we are—for the sake of the argument—to neglect m_{eff}^2 in ϵ , we may write for a single resonance $P_{\text{lin}} \sim \epsilon |g_{a\gamma}| BR$. This shows that to compensate for $\epsilon \ll 1$ one should maximize the product BR . Saturating R by the size L of the system, we estimate for the product $BL \sim 10^{-8}$ G Mpc for the Milky Way and 10^{-6} G Mpc for galaxy clusters. In the centers of clusters, the contribution from the photon-photon scattering in (4) is of the same size as the plasma frequency $\omega_p^2 \sim m_{\text{eff}}^2|_{\text{EM}}$ for GeV energies but the condition $\epsilon \ll 1$ is violated. If we look at magnetars with their extremely large magnetic field strengths $B \sim 10^{14}$ G and size $L \sim 10$ km, we find $BL \sim 10^{-4}$ G Mpc while retaining $\epsilon \ll 1$ for GHz-THz frequencies. This demonstrates that NS have a unique potential to probe the smallest values of $g_{a\gamma}$ through resonant conversion, and for the remainder of the paper we focus on this case.

Magnetosphere model and expected signal. For an estimate of the electron density we use the Goldreich-Julian (GJ) model [59] that predicts the required magnetospheric co-rotating spatial charge density n_c as the difference of positive and negative charge carriers,

$$n_c = \frac{\vec{\Omega} \cdot \vec{B}}{\sqrt{\pi\alpha}} \frac{1}{1 - \Omega^2 r^2 \sin^2 \theta}, \quad (5)$$

where $\vec{\Omega}$ is the vector along the axis of rotation with magnitude $\Omega = 2\pi/P$ the NS angular frequency (P is a rotation period); θ is the angle between \vec{r} and $\vec{\Omega}$. We then take $n_e = |n_c|$ as an estimate on the electron (or positron) number density; we caution that larger densities are sometimes considered, see [60, 61]. On the account that $\Omega r \ll 1$ out to large radii, the electron density only depends on the \hat{z} -component of the magnetic field, $n_e \simeq \Omega B |\cos \theta_B| / \sqrt{\pi \alpha}$, where θ_B is the angle between \vec{B} and $\vec{\Omega}$.

We are now in a position to study the condition $m_{\text{eff}}^2 = m_a^2$ from (4). Using $\rho_{\text{EM}} = B^2/2$, we may write it as $m_a^2 = C_1 |\cos \theta_B| B - C_2 \omega^2 B^2$ with $C_1 = \frac{4\Omega\sqrt{\pi\alpha}}{m_e}$ and $C_2 = \frac{44\alpha^2}{135m_e^4}$. Being a quadratic equation in B , we observe that resonant conversion is only possible for energies below a critical value

$$\omega_c = \frac{C_1 |\cos \theta_B|}{2m_a \sqrt{C_2}} \approx 10^{-2} \text{ eV} |\cos \theta_B| \left(\frac{1 \text{ s}}{P} \right) \left(\frac{10^{-5} \text{ eV}}{m_a} \right),$$

which also highlights that, in the GJ model, the charge density vanishes for $\cos \theta_B = 0$. For $\omega < \omega_c$ there are two physical solutions for the resonant magnetic field value. In the limit of small frequencies, the photon-photon scattering contribution can always be neglected and one obtains a resonance that is associated with a small magnetic field value at a distance from the NS surface,

$$B_- \approx \frac{m_a^2}{C_1 |\cos \theta_B|} \approx \frac{10^{12} \text{ G}}{|\cos \theta_B|} \left(\frac{P}{1 \text{ s}} \right) \left(\frac{m_a}{10^{-5} \text{ eV}} \right)^2.$$

In turn, for growing photon energy, the cancellation between plasma frequency and the photon-photon scattering term becomes possible (“double lens”). In the limit $\omega \ll \omega_c$ any parametric dependence on m_a can be neglected and the solution is given by,

$$B_+ \approx \frac{C_1 |\cos \theta_B|}{C_2 \omega^2} \approx 10^{15} \text{ G} |\cos \theta_B| \left(\frac{1 \text{ s}}{P} \right) \left(\frac{10^{-3} \text{ eV}}{\omega} \right)^2.$$

For $\omega \gtrsim 10^{-3} \text{ eV}$, the required B_+ field values are found at radii close to the magnetar’s surface. They are associated with significant efficiency of conversion and $P_{\text{tot}} \approx 1/3$ can be attained. Hence, a *sharp feature at $\omega = \omega_{\text{kink}}$ on the emanating photon flux can be imprinted once the B_+ resonance is found*. The second sharp feature is at $\omega = \omega_c$ but is difficult to access observationally; note that $\omega = 10^{-3} (10^{-2}) \text{ eV}$ corresponds to $\nu \simeq 240 \text{ GHz} (2.4 \text{ THz})$. Finally, we note that for large $g_{a\gamma}$ and m_a values, the B_- resonance may become efficient enough to deplete the photon flux already for $\omega < \omega_{\text{kink}}$, with the general effect of washing out the spectral feature at ω_{kink} ; we take this into account below.

To make progress, we may follow previous investigations [39–44] in assuming that the magnetic field is well

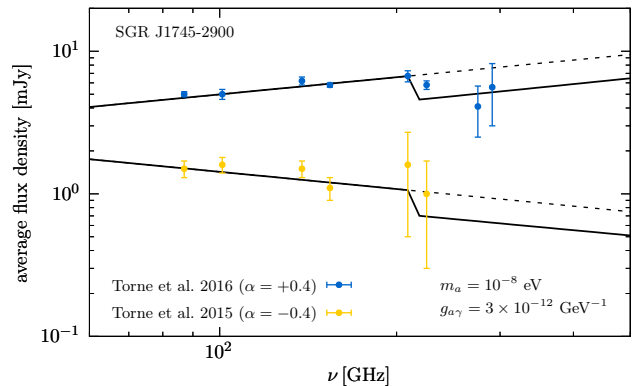


FIG. 2. High-frequency radio spectrum of SGR J1745-2900 during two observational campaigns over several days in 2014 [64] and 2015 [65] together with reported fitted power laws that include additional data points below 10 GHz (not shown.) The solid lines show the effect of photon-axion conversion for $m_a \leq 10^{-8} \text{ eV}$ and $g_{a\gamma} = 3 \times 10^{-12} \text{ GeV}^{-1}$.

described by a dipole configuration,

$$\vec{B} = \frac{1}{4\pi} \left[\frac{3\vec{r}(\vec{r} \cdot \vec{m})}{r^5} - \frac{\vec{m}}{r^3} \right], \quad (6)$$

with magnetic moment $\vec{m} = 2\pi B_0 r_0^3 \hat{n}$, where B_0 is the maximum field value at the surface of magnetic poles, $r_0 = 10 \text{ km}$ is the assumed radius of the neutron star, and \hat{n} is the unit vector along \vec{m} . Taking the star’s rotation axis along the \hat{z} -direction and the magnetic moment misaligned by an angle θ_m one arrives at $\vec{n}(t) = (\sin \theta_m \cos \Omega t, \sin \theta_m \sin \Omega t, \cos \theta_m)$. Plugging this expression into (6) yields the time-dependent magnetic field.

This model has several features. First, for lines-of-sight that end on the polar regions, the conversion probability is suppressed because of the parallel magnetic field structure, $B_T \ll B_0$. Second, the GJ model has a quadrupolar structure with directions of vanishing charge density. Both these features suggest strong geometric dependencies. However, to a certain degree, they can be considered artifacts. First, there can be toroidal and turbulent magnetic field components of comparable strength close to the NS surface [62], the region most relevant to us. Second, the actual electron density may differ from the GJ one. From Fig. 1 one observes that an increase of $n_e = 10^{13} \text{ cm}^{-3}$ by two orders of magnitude shifts the spectral break by one order of magnitude into the observationally difficult THz regime. Our proposal, therefore, hinges on electron densities that are not too different from the GJ ones paired with magnetic field values in the $10^{14} - 10^{15} \text{ G}$ ballpark, inducing a spectral break at several hundred GHz or lower. Finally, we are sensitive to the assumption that the pulsed radio signal is produced close to the NS surface—a process that is still poorly understood [63].

Having mentioned important caveats to our proposal,

we now proceed studying its sensitivity potential by making some simplifying assumptions. Importantly, in the regime where the conversion becomes saturated, $P_{\text{tot}} \approx 1/3$, all geometric dependencies are distilled into the position of the sharp feature in frequency only. In fact, the latter does not depend on direction but only on B -field magnitude at the respective region very close to the surface, and we expect ω_{kink} to remain preserved over the typical observational time windows of several hours. Therefore, for the purpose of illustration, we keep the asymptotic radial scaling of a magnetic dipole, $B = B_0(r_0/r)^3$, but take its direction to be random. We replace occurrences of the angle θ_B by its average assuming its uniform distribution: $\langle |\cos \theta_B| \rangle = 1/2$ so that $n_e = \Omega B/e$, and take $\langle \sin^2 \theta_B \rangle = 2/3$ in the conversion probability. Taken together, these assumptions allow for a simple exposition of our ideas while retaining the essential features.

SGR J1745-2900 as an exemplary source. We choose the radio-loud magnetar SGR J1745-2900, 0.1 pc near the galactic center with a period $P = 3.76$ s [66, 67] and $B_0 = 1.6 \times 10^{14}$ G [67] as an exemplary source. Its pulsed radio emissions with mJy flux density have been measured over an unprecedented broad range from 2.54 GHz (118 mm) up to 225 GHz (1.33 mm) [64] and to 291 GHz (1.03 mm) [65] over a period of several days in 2014 and 2015, respectively. The observed mean spectral densities were relatively flat, with respective power law indices $\langle \alpha \rangle = -0.4 \pm 0.1$ and $\langle \alpha \rangle = +0.4 \pm 0.2$, with a possibility of a spectral break at tens of GHz. Flux density and spectral index variabilities are observed on long and short time scales. The details of pulsed (radio) emission from magnetars remain poorly understood but are generally expected to be associated with open field lines of polar regions [68].¹

Figure 2 shows the averaged radio spectral densities of SGR J1745-2900 as a function of frequency of the two observational campaigns over several days in 2014 [64] and 2015 [64]. The dashed lines show the reported fitted power laws (which are additionally anchored by low-frequency data from 1-10 GHz.) The solid green line is obtained by multiplying the fits by $1 - P_{\text{tot}}$ for $m_a = 10^{-8}$ eV and $g_{a\gamma} = 3 \times 10^{-12}$ GeV using the simplified magnetospheric model described above. As can be seen, for $\nu \gtrsim 200$ GHz, the resonance associated with B_+ can be met, leading to a sharp saturated reduction of the flux by a factor one third.

¹ There is evidence for some degree of linear polarization up to the highest frequencies [65]. It is well known that the photon-photon scattering contribution is birefringent [69, 70] and that the electric field of the converted radio wave is aligned with the tangential component B_T . This may induce $O(1)$ variations within a pulse, which we are not able to resolve at the current state. A study of polarization effects is left for future work.

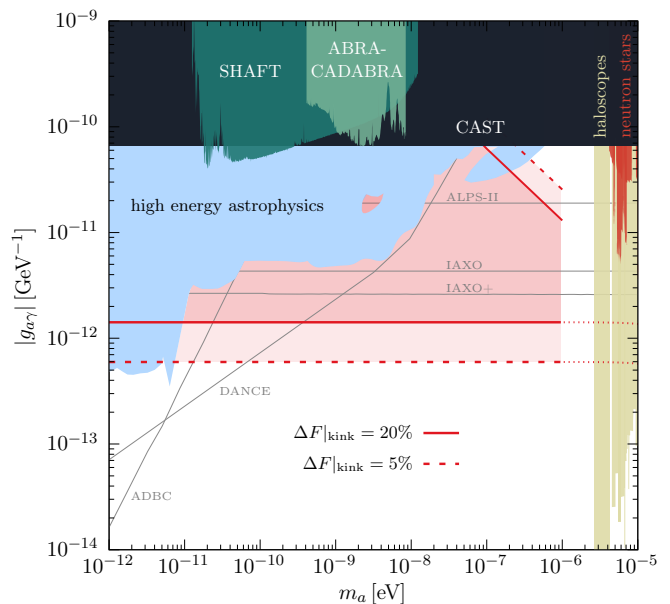


FIG. 3. Sensitivity region on photon-ALP resonant conversion bounded by the solid (dashed) red line based on the assumption that a 20% (5%) spectral feature can be detected. Astrophysical constraints are cumulatively shown by the blue shaded region labeled “high energy astrophysics” (see [71]). Laboratory limits from CAST [72], SHAFT [73], ABRACADABRA [74] and projections for ALPS-II [75], IAXO(+) [76], DANCE [77], and ADBC [78] are shown as labeled. Additional constraints that assume ALPs being DM are from haloscopes [79–85] and previous analyses using neutron stars [42, 43, 46].

Figure 3 explores the sensitivity in the $(m_a, |g_{a\gamma}|)$ plane to resonant conversion assuming that a sharp spectral feature, i.e., a sudden flux reduction $\Delta F|_{\text{kink}}$ can be detected at the frequency where B_+ becomes available. The solid (dashed) red line depicts $\Delta F|_{\text{kink}} = 20\%$ (5%). As can be seen, for $m_a \lesssim 10^{-5}$ eV, the result is independent of axion mass and a sensitivity as good as $|g_{a\gamma}| \lesssim 1.4 \times 10^{-12}$ (6×10^{-13}) GeV⁻¹ can be reached. For $m_a \gtrsim 10^{-6}$ eV and/or for large $|g_{a\gamma}|$, the conversion associated with B_- is strong enough to deplete the photon flux for frequencies below the onset of B_+ . This washes out the kink and the red shading indicates the region unaffected by it. Existing ALP constraints and other laboratory projections are additionally shown as labeled. As can be seen, an improvement over current limits by more than an order of magnitude is possible, putting astrophysics in competition with upcoming laboratory searches that target a wide range of ALP masses, in particular from 10^{-11} eV to 10^{-6} eV.

Conclusions. In this work, we show that observations of the high-frequency end of the radio band of magnetars host the possibility to put very stringent constraints on the ALP-photon coupling from resonant conversion at the 10^{-12} GeV⁻¹ level. The method works for an arbitrary

trarily small and hence wide range of m_a , leveraging the energy-dependent negative contribution from the radiation field to the effective photon mass (“double lens effect”). It removes the direct relation between axion mass and resonant electron number density and, at the same time, places the resonance radius close to the neutron star surface with ensuing strong conversion probability. Because of the sharp NS surface boundary, a spectral feature that can be searched for in high-quality radio data is imprinted.

Currently, an incomplete understanding of the magnetospheres’ physical conditions and the ensuing production and propagation of radio photons from there prevents us from claiming real limits. However, many uncertainties are expected to be mitigated by future observations with SKA [86–90], complemented by the steady stream of high-frequency observations in the few hundred GHz range by mm/sub-mm arrays such as ALMA, IRAM, or JCMT [91–93], and through paralleling advances in the simulation and modeling of these extreme objects [94–100]. Together, photon-axion conversion in neutron stars may well become a serious competitor to the experimental ALPS-II and IAXO programs.

Acknowledgements. We thank Yuri Levin and Andrii Neronov for helpful discussions. KB is partly funded by the INFN PD51 INDARK grant. AB is supported by the European Research Council (ERC) Advanced Grant “NuBSM” (694896). AS is supported by the Kavli Institute for Cosmological Physics at the University of Chicago through an endowment from the Kavli Foundation and its founder Fred Kavli. This work has been supported by the Fermi Research Alliance, LLC under Contract No. DE-AC02-07CH11359 with the U.S. Department of Energy, Office of High Energy Physics.

* kyrylo.bondarenko@cern.ch

† boyarsky@lorentz.leidenuniv.nl

‡ josef.pradler@oeaw.ac.at

§ sokolenko@kicp.uchicago.edu

- [1] R. D. Peccei and H. R. Quinn, CP Conservation in the Presence of Instantons, *Phys. Rev. Lett.* **38**, 1440 (1977).
- [2] R. D. Peccei and H. R. Quinn, Constraints Imposed by CP Conservation in the Presence of Instantons, *Phys. Rev. D* **16**, 1791 (1977).
- [3] S. Weinberg, A New Light Boson?, *Phys. Rev. Lett.* **40**, 223 (1978).
- [4] F. Wilczek, Problem of Strong P and T Invariance in the Presence of Instantons, *Phys. Rev. Lett.* **40**, 279 (1978).
- [5] J. E. Kim, Weak Interaction Singlet and Strong CP Invariance, *Phys. Rev. Lett.* **43**, 103 (1979).
- [6] M. A. Shifman, A. I. Vainshtein, and V. I. Zakharov, Can Confinement Ensure Natural CP Invariance of Strong Interactions?, *Nucl. Phys. B* **166**, 493 (1980).
- [7] A. R. Zhitnitsky, On Possible Suppression of the Axion Hadron Interactions. (In Russian), *Sov. J. Nucl. Phys.* **31**, 260 (1980).
- [8] M. Dine, W. Fischler, and M. Srednicki, A Simple Solution to the Strong CP Problem with a Harmless Axion, *Phys. Lett. B* **104**, 199 (1981).
- [9] J. Preskill, M. B. Wise, and F. Wilczek, Cosmology of the Invisible Axion, *Phys. Lett. B* **120**, 127 (1983).
- [10] L. F. Abbott and P. Sikivie, A Cosmological Bound on the Invisible Axion, *Phys. Lett. B* **120**, 133 (1983).
- [11] M. Dine and W. Fischler, The Not So Harmless Axion, *Phys. Lett. B* **120**, 137 (1983).
- [12] P. Svrcek and E. Witten, Axions In String Theory, *JHEP* **06**, 051, [arXiv:hep-th/0605206](https://arxiv.org/abs/hep-th/0605206).
- [13] A. Arvanitaki, S. Dimopoulos, S. Dubovsky, N. Kaloper, and J. March-Russell, String Axiverse, *Phys. Rev. D* **81**, 123530 (2010), [arXiv:0905.4720](https://arxiv.org/abs/0905.4720) [hep-th].
- [14] B. S. Acharya, K. Bobkov, and P. Kumar, An M Theory Solution to the Strong CP Problem and Constraints on the Axiverse, *JHEP* **11**, 105, [arXiv:1004.5138](https://arxiv.org/abs/1004.5138) [hep-th].
- [15] A. Ringwald, Searching for axions and ALPs from string theory, *J. Phys. Conf. Ser.* **485**, 012013 (2014), [arXiv:1209.2299](https://arxiv.org/abs/1209.2299) [hep-ph].
- [16] M. Kamionkowski, J. Pradler, and D. G. E. Walker, Dark energy from the string axiverse, *Phys. Rev. Lett.* **113**, 251302 (2014), [arXiv:1409.0549](https://arxiv.org/abs/1409.0549) [hep-ph].
- [17] M. J. Stott, D. J. E. Marsh, C. Pongkitivanichkul, L. C. Price, and B. S. Acharya, Spectrum of the axion dark sector, *Phys. Rev. D* **96**, 083510 (2017), [arXiv:1706.03236](https://arxiv.org/abs/1706.03236) [astro-ph.CO].
- [18] J. Halverson, C. Long, B. Nelson, and G. Salinas, Towards string theory expectations for photon couplings to axionlike particles, *Phys. Rev. D* **100**, 106010 (2019), [arXiv:1909.05257](https://arxiv.org/abs/1909.05257) [hep-th].
- [19] G. G. Raffelt, Astrophysical axion bounds, *Lect. Notes Phys.* **741**, 51 (2008), [arXiv:hep-ph/0611350](https://arxiv.org/abs/hep-ph/0611350).
- [20] J. Jaeckel and A. Ringwald, The Low-Energy Frontier of Particle Physics, *Ann. Rev. Nucl. Part. Sci.* **60**, 405 (2010), [arXiv:1002.0329](https://arxiv.org/abs/1002.0329) [hep-ph].
- [21] P. W. Graham, I. G. Irastorza, S. K. Lamoreaux, A. Lindner, and K. A. van Bibber, Experimental Searches for the Axion and Axion-Like Particles, *Ann. Rev. Nucl. Part. Sci.* **65**, 485 (2015), [arXiv:1602.00039](https://arxiv.org/abs/1602.00039) [hep-ex].
- [22] D. J. E. Marsh, Axion Cosmology, *Phys. Rept.* **643**, 1 (2016), [arXiv:1510.07633](https://arxiv.org/abs/1510.07633) [astro-ph.CO].
- [23] I. G. Irastorza and J. Redondo, New experimental approaches in the search for axion-like particles, *Prog. Part. Nucl. Phys.* **102**, 89 (2018), [arXiv:1801.08127](https://arxiv.org/abs/1801.08127) [hep-ph].
- [24] G. G. Raffelt, Astrophysical methods to constrain axions and other novel particle phenomena, *Phys. Rept.* **198**, 1 (1990).
- [25] M. Giannotti, I. G. Irastorza, J. Redondo, A. Ringwald, and K. Saikawa, Stellar Recipes for Axion Hunters, *JCAP* **10**, 010, [arXiv:1708.02111](https://arxiv.org/abs/1708.02111) [hep-ph].
- [26] C. Dessert, J. W. Foster, and B. R. Safdi, X-ray Searches for Axions from Super Star Clusters, *Phys. Rev. Lett.* **125**, 261102 (2020), [arXiv:2008.03305](https://arxiv.org/abs/2008.03305) [hep-ph].
- [27] M. Xiao, K. M. Perez, M. Giannotti, O. Straniero, A. Mirizzi, B. W. Grefenstette, B. M. Roach, and M. Nynka, Constraints on Axionlike Particles from a Hard X-Ray Observation of Betelgeuse, *Phys. Rev. Lett.* **126**, 031101 (2021), [arXiv:2009.09059](https://arxiv.org/abs/2009.09059) [astro-ph.HE].

- [28] A. Payez, C. Evoli, T. Fischer, M. Giannotti, A. Mirizzi, and A. Ringwald, Revisiting the SN1987A gamma-ray limit on ultralight axion-like particles, *JCAP* **02**, 006, [arXiv:1410.3747 \[astro-ph.HE\]](#).
- [29] A. Mirizzi, G. G. Raffelt, and P. D. Serpico, Signatures of Axion-Like Particles in the Spectra of TeV Gamma-Ray Sources, *Phys. Rev. D* **76**, 023001 (2007), [arXiv:0704.3044 \[astro-ph\]](#).
- [30] D. Hooper and P. D. Serpico, Detecting Axion-Like Particles With Gamma Ray Telescopes, *Phys. Rev. Lett.* **99**, 231102 (2007), [arXiv:0706.3203 \[hep-ph\]](#).
- [31] K. A. Hochmuth and G. Sigl, Effects of Axion-Photon Mixing on Gamma-Ray Spectra from Magnetized Astrophysical Sources, *Phys. Rev. D* **76**, 123011 (2007), [arXiv:0708.1144 \[astro-ph\]](#).
- [32] A. De Angelis, O. Mansutti, and M. Roncadelli, Axion-Like Particles, Cosmic Magnetic Fields and Gamma-Ray Astrophysics, *Phys. Lett. B* **659**, 847 (2008), [arXiv:0707.2695 \[astro-ph\]](#).
- [33] A. De Angelis, M. Roncadelli, and O. Mansutti, Evidence for a new light spin-zero boson from cosmological gamma-ray propagation?, *Phys. Rev. D* **76**, 121301 (2007), [arXiv:0707.4312 \[astro-ph\]](#).
- [34] D. Horns, L. Maccione, M. Meyer, A. Mirizzi, D. Montanino, and M. Roncadelli, Hardening of TeV gamma spectrum of AGNs in galaxy clusters by conversions of photons into axion-like particles, *Phys. Rev. D* **86**, 075024 (2012), [arXiv:1207.0776 \[astro-ph.HE\]](#).
- [35] M. Berg, J. P. Conlon, F. Day, N. Jennings, S. Krippendorf, A. J. Powell, and M. Rummel, Constraints on Axion-Like Particles from X-ray Observations of NGC1275, *Astrophys. J.* **847**, 101 (2017), [arXiv:1605.01043 \[astro-ph.HE\]](#).
- [36] C. S. Reynolds, M. C. D. Marsh, H. R. Russell, A. C. Fabian, R. Smith, F. Tombesi, and S. Veilleux, Astrophysical limits on very light axion-like particles from Chandra grating spectroscopy of NGC 1275, *ApJ* **890**, 10.3847/1538-4357/ab6a0c (2019), [arXiv:1907.05475 \[hep-ph\]](#).
- [37] M. C. D. Marsh, H. R. Russell, A. C. Fabian, B. P. McNamara, P. Nulsen, and C. S. Reynolds, A New Bound on Axion-Like Particles, *JCAP* **12**, 036, [arXiv:1703.07354 \[hep-ph\]](#).
- [38] A. Hook, Y. Kahn, B. R. Safdi, and Z. Sun, Radio Signals from Axion Dark Matter Conversion in Neutron Star Magnetospheres, *Phys. Rev. Lett.* **121**, 241102 (2018), [arXiv:1804.03145 \[hep-ph\]](#).
- [39] M. S. Pshirkov and S. B. Popov, Conversion of Dark matter axions to photons in magnetospheres of neutron stars, *J. Exp. Theor. Phys.* **108**, 384 (2009), [arXiv:0711.1264 \[astro-ph\]](#).
- [40] F. P. Huang, K. Kadota, T. Sekiguchi, and H. Tashiro, Radio telescope search for the resonant conversion of cold dark matter axions from the magnetized astrophysical sources, *Phys. Rev. D* **97**, 123001 (2018), [arXiv:1803.08230 \[hep-ph\]](#).
- [41] B. R. Safdi, Z. Sun, and A. Y. Chen, Detecting Axion Dark Matter with Radio Lines from Neutron Star Populations, *Phys. Rev. D* **99**, 123021 (2019), [arXiv:1811.01020 \[astro-ph.CO\]](#).
- [42] J. W. Foster, Y. Kahn, O. Macias, Z. Sun, R. P. Eatough, V. I. Kondratiev, W. M. Peters, C. Weniger, and B. R. Safdi, Green Bank and Effelsberg Radio Telescope Searches for Axion Dark Matter Conversion in Neutron Star Magnetospheres, *Phys. Rev. Lett.* **125**, 171301 (2020), [arXiv:2004.00011 \[astro-ph.CO\]](#).
- [43] J. Darling, Search for Axionic Dark Matter Using the Magnetar PSR J1745-2900, *Phys. Rev. Lett.* **125**, 121103 (2020), [arXiv:2008.01877 \[astro-ph.CO\]](#).
- [44] R. A. Battye, B. Garbrecht, J. I. McDonald, and S. Srinivasan, Radio line properties of axion dark matter conversion in neutron stars, *JHEP* **09**, 105, [arXiv:2104.08290 \[hep-ph\]](#).
- [45] S. J. Witte, D. Noordhuis, T. D. P. Edwards, and C. Weniger, Axion-photon conversion in neutron star magnetospheres: The role of the plasma in the Goldreich-Julian model, *Phys. Rev. D* **104**, 103030 (2021), [arXiv:2104.07670 \[hep-ph\]](#).
- [46] R. A. Battye, J. Darling, J. McDonald, and S. Srinivasan, Towards Robust Constraints on Axion Dark Matter using PSR J1745-2900, (2021), [arXiv:2107.01225 \[astro-ph.CO\]](#).
- [47] A. J. Millar, S. Baum, M. Lawson, and M. C. D. Marsh, Axion-photon conversion in strongly magnetised plasmas, *JCAP* **11**, 013, [arXiv:2107.07399 \[hep-ph\]](#).
- [48] G. Raffelt and L. Stodolsky, Mixing of the Photon with Low Mass Particles, *Phys. Rev. D* **37**, 1237 (1988).
- [49] E. Braaten and D. Segel, Neutrino energy loss from the plasma process at all temperatures and densities, *Phys. Rev. D* **48**, 1478 (1993), [arXiv:hep-ph/9302213](#).
- [50] A. Dobrynina, A. Kartavtsev, and G. Raffelt, Photon-photon dispersion of TeV gamma rays and its role for photon-ALP conversion, *Phys. Rev. D* **91**, 083003 (2015), [Erratum: *Phys.Rev.D* 95, 109905 (2017)], [arXiv:1412.4777 \[astro-ph.HE\]](#).
- [51] K. Bondarenko, A. Boyarsky, J. Pradler, and A. Sokoleno, , in [preparation](#).
- [52] C. L. Sarazin, X-ray emission from clusters of galaxies, *Rev. Mod. Phys.* **58**, 1 (1986).
- [53] A. A. Garcia, K. Bondarenko, S. Ploeckinger, J. Pradler, and A. Sokoleno, Effective photon mass and (dark) photon conversion in the inhomogeneous Universe, *JCAP* **10**, 011, [arXiv:2003.10465 \[astro-ph.CO\]](#).
- [54] P. Sikivie, Experimental Tests of the Invisible Axion, *Phys. Rev. Lett.* **51**, 1415 (1983), [Erratum: *Phys.Rev.Lett.* 52, 695 (1984)].
- [55] P. Sikivie, Detection Rates for 'Invisible' Axion Searches, *Phys. Rev. D* **32**, 2988 (1985), [Erratum: *Phys.Rev.D* 36, 974 (1987)].
- [56] M. Schlederer and G. Sigl, Constraining ALP-photon coupling using galaxy clusters, *JCAP* **01**, 038, [arXiv:1507.02855 \[hep-ph\]](#).
- [57] A. Caputo, H. Liu, S. Mishra-Sharma, and J. T. Ruderman, Modeling Dark Photon Oscillations in Our Inhomogeneous Universe, *Phys. Rev. D* **102**, 103533 (2020), [arXiv:2004.06733 \[astro-ph.CO\]](#).
- [58] Y. Grossman, S. Roy, and J. Zupan, Effects of initial axion production and photon axion oscillation on type Ia supernova dimming, *Phys. Lett. B* **543**, 23 (2002), [arXiv:hep-ph/0204216](#).
- [59] P. Goldreich and W. H. Julian, Pulsar Electrodynamics, *ApJ* **157**, 869 (1969).
- [60] M. Lyutikov, Neutron star magnetospheres: The binary pulsar, Crab and magnetars, *AIP Conf. Proc.* **968**, 77 (2008), [arXiv:0708.1024 \[astro-ph\]](#).
- [61] D. N. Sob'yanin, Breakdown of the Goldreich-Julian Relation in a Neutron Star, *Astron. Lett.* **42**, 745 (2016), [arXiv:1612.09139 \[astro-ph.HE\]](#).

- [62] V. M. Kaspi and A. Beloborodov, Magnetars, *Ann. Rev. Astron. Astrophys.* **55**, 261 (2017), [arXiv:1703.00068 \[astro-ph.HE\]](#).
- [63] R. Turolla, S. Zane, and A. Watts, Magnetars: the physics behind observations. A review, *Rept. Prog. Phys.* **78**, 116901 (2015), [arXiv:1507.02924 \[astro-ph.HE\]](#).
- [64] P. Torne *et al.*, Simultaneous multifrequency radio observations of the Galactic Centre magnetar SGR J1745–2900, *Mon. Not. Roy. Astron. Soc.* **451**, L50 (2015), [arXiv:1504.07241 \[astro-ph.HE\]](#).
- [65] P. Torne, G. Desvignes, R. P. Eatough, R. Karuppusamy, G. Paubert, M. Kramer, I. Cognard, D. J. Champion, and L. G. Spitler, Detection of the magnetar SGR J1745–2900 up to 291 GHz with evidence of polarized millimetre emission, *Mon. Not. Roy. Astron. Soc.* **465**, 242 (2017), [arXiv:1610.07616 \[astro-ph.HE\]](#).
- [66] J. A. Kennea *et al.*, Swift Discovery of a New Soft Gamma Repeater, SGR J1745-29, near Sagittarius A*, *Astrophys. J. Lett.* **770**, L24 (2013), [arXiv:1305.2128 \[astro-ph.HE\]](#).
- [67] K. Mori *et al.*, NuSTAR discovery of a 3.76-second transient magnetar near Sagittarius A*, *Astrophys. J. Lett.* **770**, L23 (2013), [arXiv:1305.1945 \[astro-ph.HE\]](#).
- [68] A. M. Beloborodov, Untwisting magnetospheres of neutron stars, *Astrophys. J.* **703**, 1044 (2009), [arXiv:0812.4873 \[astro-ph\]](#).
- [69] W.-y. Tsai and T. Erber, Photon Pair Creation in Intense Magnetic Fields, *Phys. Rev. D* **10**, 492 (1974).
- [70] W.-y. Tsai and T. Erber, The Propagation of Photons in Homogeneous Magnetic Fields: Index of Refraction, *Phys. Rev. D* **12**, 1132 (1975).
- [71] C. O’Hare, Axionlimits, <https://github.com/cajohare/AxionLimits> (2021).
- [72] V. Anastassopoulos *et al.* (CAST), New CAST Limit on the Axion-Photon Interaction, *Nature Phys.* **13**, 584 (2017), [arXiv:1705.02290 \[hep-ex\]](#).
- [73] A. V. Gramolin, D. Aybas, D. Johnson, J. Adam, and A. O. Sushkov, Search for axion-like dark matter with ferromagnets, *Nature Phys.* **17**, 79 (2021), [arXiv:2003.03348 \[hep-ex\]](#).
- [74] C. P. Salemi *et al.*, The search for low-mass axion dark matter with ABRACADABRA-10cm, (2021), [arXiv:2102.06722 \[hep-ex\]](#).
- [75] M. D. Ortiz *et al.*, Design of the ALPS II optical system, *Phys. Dark Univ.* **35**, 100968 (2022), [arXiv:2009.14294 \[physics.optics\]](#).
- [76] I. Shilon, A. Dudarev, H. Silva, and H. H. J. ten Kate, Conceptual Design of a New Large Superconducting Toroid for IAXO, the New International AXion Observatory, *IEEE Transactions on Applied Superconductivity* **23**, 4500604 (2013), [arXiv:1212.4633 \[physics.ins-det\]](#).
- [77] Y. Michimura, Y. Oshima, T. Watanabe, T. Kawasaki, H. Takeda, M. Ando, K. Nagano, I. Obata, and T. Fujita, DANCE: Dark matter Axion search with riNg Cavity Experiment, *J. Phys. Conf. Ser.* **1468**, 012032 (2020), [arXiv:1911.05196 \[physics.ins-det\]](#).
- [78] H. Liu, B. D. Elwood, M. Evans, and J. Thaler, Searching for Axion Dark Matter with Birefringent Cavities, *Phys. Rev. D* **100**, 023548 (2019), [arXiv:1809.01656 \[hep-ph\]](#).
- [79] S. DePanfilis, A. C. Melissinos, B. E. Moskowitz, J. T. Rogers, Y. K. Semertzidis, W. U. Wuensch, H. J. Halam, A. G. Prodel, W. B. Fowler, and F. A. Nezrick, Limits on the abundance and coupling of cosmic axions at $4.5 < m_a < 5.0 \mu\text{eV}$, *Phys. Rev. Lett.* **59**, 839 (1987).
- [80] L. Zhong *et al.* (HAYSTAC), Results from phase 1 of the HAYSTAC microwave cavity axion experiment, *Phys. Rev. D* **97**, 092001 (2018), [arXiv:1803.03690 \[hep-ex\]](#).
- [81] T. Braine *et al.* (ADMX), Extended Search for the Invisible Axion with the Axion Dark Matter Experiment, *Phys. Rev. Lett.* **124**, 101303 (2020), [arXiv:1910.08638 \[hep-ex\]](#).
- [82] K. M. Backes *et al.* (HAYSTAC), A quantum-enhanced search for dark matter axions, *Nature* **590**, 238 (2021), [arXiv:2008.01853 \[quant-ph\]](#).
- [83] J. Jeong, S. Youn, S. Bae, J. Kim, T. Seong, J. E. Kim, and Y. K. Semertzidis, Search for Invisible Axion Dark Matter with a Multiple-Cell Haloscope, *Phys. Rev. Lett.* **125**, 221302 (2020), [arXiv:2008.10141 \[hep-ex\]](#).
- [84] S. Lee, S. Ahn, J. Choi, B. R. Ko, and Y. K. Semertzidis, Axion Dark Matter Search around $6.7 \mu\text{eV}$, *Phys. Rev. Lett.* **124**, 101802 (2020), [arXiv:2001.05102 \[hep-ex\]](#).
- [85] C. Bartram *et al.* (ADMX), Search for Invisible Axion Dark Matter in the $3.3\text{--}4.2 \mu\text{eV}$ Mass Range, *Phys. Rev. Lett.* **127**, 261803 (2021), [arXiv:2110.06096 \[hep-ex\]](#).
- [86] M. Kramer, A. G. Lyne, J. T. O’Brien, C. A. Jordan, and D. R. Lorimer, A periodically active pulsar giving insight into magnetospheric physics, *Science* **312**, 549 (2006), [arXiv:astro-ph/0604605](#).
- [87] A. Watts *et al.*, Understanding the Neutron Star Population with the SKA, *PoS AASKA14*, 039 (2015), [arXiv:1501.00005 \[astro-ph.HE\]](#).
- [88] E. F. Keane *et al.*, A Cosmic Census of Radio Pulsars with the SKA, *PoS AASKA14*, 040 (2015), [arXiv:1501.00056 \[astro-ph.IM\]](#).
- [89] A. Karastergiou *et al.*, Understanding pulsar magnetospheres with the SKA, *PoS AASKA14*, 038 (2015), [arXiv:1501.00126 \[astro-ph.HE\]](#).
- [90] J. Antoniadis, L. Guillemot, A. Possenti, S. Bogdanov, J. Gelfand, M. Kramer, R. Mignani, B. Stappers, and P. Torne, Multi-wavelength, Multi-Messenger Pulsar Science in the SKA Era, *PoS AASKA14*, 157 (2015), [arXiv:1501.05591 \[astro-ph.HE\]](#).
- [91] C.-Y. Chu, C. Y. Ng, A. K. H. Kong, and H.-K. Chang, High-frequency radio observations of two magnetars, PSR J1622 – 4950 and 1E 1547.0 – 5408, *Mon. Not. Roy. Astron. Soc.* **503**, 1214 (2021), [arXiv:2102.02466 \[astro-ph.HE\]](#).
- [92] P. Torne *et al.*, Searching for pulsars in the Galactic centre at 3 and 2 mm, *Astron. Astrophys.* **650**, A95 (2021), [arXiv:2103.16581 \[astro-ph.HE\]](#).
- [93] P. Torne *et al.*, Submillimeter Pulsations from the Magnetar XTE J1810-197, *Astrophys. J. Lett.* **925**, L17 (2022), [arXiv:2201.07820 \[astro-ph.HE\]](#).
- [94] A. A. Philippov, A. Spitkovsky, and B. Cerutti, Ab-initio pulsar magnetosphere: three-dimensional particle-in-cell simulations of oblique pulsars, *Astrophys. J. Lett.* **801**, L19 (2015), [arXiv:1412.0673 \[astro-ph.HE\]](#).
- [95] J. Pétri, Theory of pulsar magnetosphere and wind, *J. Plasma Phys.* **82**, 635820502 (2016), [arXiv:1608.04895 \[astro-ph.HE\]](#).
- [96] A. Y. Chen and A. M. Beloborodov, Particle-in-cell simulations of the twisted magnetospheres of magnetars. I, *Astrophys. J.* **844**, 133 (2017), [arXiv:1610.10036 \[astro-ph.HE\]](#).

- [97] B. Cerutti and A. Beloborodov, Electrodynamics of pulsar magnetospheres, *Space Sci. Rev.* **207**, 111 (2017), [arXiv:1611.04331 \[astro-ph.HE\]](#).
- [98] G. Brambilla, C. Kalapotharakos, A. Timokhin, A. Harding, and D. Kazanas, Electron–Positron Pair Flow and Current Composition in the Pulsar Magnetosphere, *Astrophys. J.* **858**, 81 (2018), [arXiv:1710.03536 \[astro-ph.HE\]](#).
- [99] F. Carrasco and M. Shibata, Magnetosphere of an orbiting neutron star, *Phys. Rev. D* **101**, 063017 (2020), [arXiv:2001.04210 \[astro-ph.HE\]](#).
- [100] A. Y. Chen, F. Cruz, and A. Spitkovsky, Filling the Magnetospheres of Weak Pulsars, *ApJ* **889**, 69 (2020), [arXiv:1911.00059 \[astro-ph.HE\]](#).